
Three flavor neutrino oscillation analysis of the Superkamiokande atmospheric neutrino data

Osamu Yasuda

*Department of Physics, Tokyo Metropolitan University,
1-1 Minami-Osawa Hachioji, Tokyo 192-0397, Japan,
yasuda@phys.metro-u.ac.jp*

Abstract

Superkamiokande atmospheric neutrino data for 414 days are analyzed in the framework of three flavor oscillations with mass hierarchy. It is shown that the best fit point is very close to the pure maximal $\nu_\mu \leftrightarrow \nu_\tau$ case and $\Delta m^2 \simeq 7 \times 10^{-3}$ eV². The allowed region at 90 %CL is given and the implications to the long baseline experiments are briefly discussed. It is also shown that the threefold maximal mixing model fits to the data of atmospheric neutrinos and the reactor experiments for $\Delta m^2 \sim 1 \times 10^{-3}$ eV².

1. Introduction

Recent atmospheric neutrino data of the Superkamiokande experiment^{11,12,17} provide very strong evidence for neutrino oscillations. The original analysis by the Superkamiokande group is based on the two flavor framework. Despite the constraints from the reactor experiments^{27,1,2}, there can be small mixing between ν_μ and ν_e in the atmospheric neutrinos. To estimate the oscillation probability of $\nu_e \leftrightarrow \nu_x$ or $\bar{\nu}_e \leftrightarrow \bar{\nu}_x$ in the long baseline experiments^{23,21,16,25,26}, therefore, it is important to know the allowed region of the mixing parameters at a certain confidence level. In this talk I present a three flavor analysis of the Superkamiokande atmospheric neutrino data for 414 days¹¹. Some of the contents of this presentation overlaps with Lisi's talk^{18,7}.

2. Three flavor analysis of the Superkamiokande atmospheric neutrino data

To evaluate the number of events, we integrate numerically the Schrödinger equation

$$i \frac{d}{dx} \begin{pmatrix} \nu_e(x) \\ \nu_\mu(x) \\ \nu_\tau(x) \end{pmatrix} = \left[U \text{diag}(0, \Delta E_{21}, \Delta E_{31}) U^{-1} + \text{diag}(A, 0, 0) \right] \begin{pmatrix} \nu_e(x) \\ \nu_\mu(x) \\ \nu_\tau(x) \end{pmatrix}, \quad (1)$$

where

$$U \equiv \begin{pmatrix} U_{e1} & U_{e2} & U_{e3} \\ U_{\mu 1} & U_{\mu 2} & U_{\mu 3} \\ U_{\tau 1} & U_{\tau 2} & U_{\tau 3} \end{pmatrix}$$

is the MNS mixing matrix¹⁹, E is the neutrino energy, $A \equiv \sqrt{2}G_F N_e(x)$ stands for the matter effect^{20,28} in the Earth, $\Delta E_{ij} \equiv \Delta m_{ij}^2/2E$, $\Delta m_{ij}^2 \equiv m_i^2 - m_j^2$. We assume without loss of generality that Δm_{21}^2 has the smallest absolute value of the mass squared difference. To account for the solar neutrino deficit³ we assume that Δm_{21}^2 is of order 10^{-5}eV^2 or $10^{-10} - 10^{-9}\text{eV}^2$. On the other hand, the zenith angle dependence in the atmospheric neutrino anomaly requires that the larger mass squared difference be of order $10^{-3} - 10^{-2}\text{eV}^2$. So the pattern of the mass squared differences has hierarchy and can be classified into two cases which are depicted in Fig. 1.

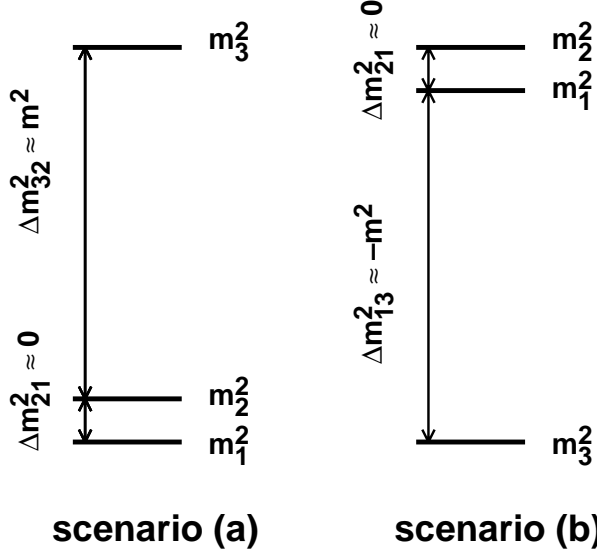


Fig. 1 The hierarchical neutrino mass squared differences. The scenarios (a) and (b) are related by exchanging $m^2 \leftrightarrow -m^2$. They are equivalent in vacuum but physically inequivalent in matter.

The eigenvalues of the Schrödinger equation (1) are given by⁴

$$\begin{cases} \alpha/3 + (2/3)\sqrt{\alpha^2 - 3\beta} \cos(\chi/3) \\ \alpha/3 - (2/3)\sqrt{\alpha^2 - 3\beta} \cos((\chi - \pi)/3) \\ \alpha/3 - (2/3)\sqrt{\alpha^2 - 3\beta} \cos((\chi + \pi)/3), \end{cases} \quad (2)$$

where

$$\begin{aligned} \chi &\equiv \cos^{-1} \left[\frac{2\alpha^3 - 9\alpha\beta + 27\gamma}{2(\alpha^2 - 3\beta)^{3/2}} \right] \\ \alpha &\equiv \Delta E_{31} + \Delta E_{21} + A \\ \beta &\equiv \Delta E_{31}\Delta E_{21} + A \left[\Delta E_{31}(1 - |U_{e3}|^2) + \Delta E_{21}(1 - |U_{e2}|^2) \right] \\ \gamma &\equiv \Delta E_{31}\Delta E_{21}A|U_{e1}|^2 \end{aligned}$$

Under our assumption that $\Delta m^2 \lesssim 10^{-5}\text{eV}^2$, in the contained atmospheric neutrino events ($0.1 \text{ GeV} \leq E \leq 100 \text{ GeV}$) we have $|\Delta E_{21}L| \ll 1$ for downward going events (L is the neutrino path length and $L \lesssim 500 \text{ km}$), and $|\Delta E_{31}|$, $|\Delta E_{32}|$, $A \gg |\Delta E_{21}|$ for upward going events. Thus the eigenvalues in (2) with $\Delta m_{21}^2 \sim \mathcal{O}(10^{-5}\text{eV}^2)$ or $\mathcal{O}(10^{-10}\text{eV}^2)$ are almost the same as those with $\Delta m_{21}^2 \equiv 0$ to good precision, i.e., *the matter effects are much more important than the smaller mass squared difference $\Delta m_{21}^2 \lesssim 10^{-5}\text{eV}^2$ in the atmospheric neutrino problem*. Hence we can safely ignore Δm_{21}^2 in the following discussions. In the limit $\Delta m_{21}^2 = 0$ the mass matrix on the right hand side of (1) becomes

$$D \left[U(\theta_{12} = \delta = 0) \text{diag}(0, 0, \Delta E_{31}) U^{-1}(\theta_{12} = \delta = 0) + \text{diag}(A, 0, 0) \right] D^{-1}, \quad (3)$$

where $D \equiv \text{diag}(e^{-i\delta}, 1, 1)$, we have used the standard parametrization²⁴ of the MNS mixing matrix¹⁹

$$U \equiv e^{i\theta_{23}\lambda_7} \text{diag}(e^{-i\delta/2}, 1, e^{i\delta/2}) e^{i\theta_{13}\lambda_5} \text{diag}(e^{i\delta/2}, 1, e^{-i\delta/2}) e^{i\theta_{12}\lambda_2}$$

and

$$\lambda_2 = \begin{pmatrix} 0 & -i & 0 \\ i & 0 & 0 \\ 0 & 0 & 1 \end{pmatrix}, \quad \lambda_5 = \begin{pmatrix} 0 & 0 & -i \\ 0 & 1 & 0 \\ i & 0 & 0 \end{pmatrix}, \quad \lambda_7 = \begin{pmatrix} 1 & 0 & 0 \\ 0 & 0 & -i \\ 0 & i & 0 \end{pmatrix},$$

are the Gell-Mann matrices. As we see in (3), θ_{12} drops out and so does δ , as δ appears only in the overall phase of the oscillation amplitude $A(\nu_\alpha \rightarrow \nu_\beta)$. Putting $m^2 \equiv \Delta m_{31}^2$, therefore, we are left with the three parameters ($m^2, \theta_{13}, \theta_{23}$).

The way to obtain the numbers of events is exactly the same as in Foot et al.⁸, and we refer to Foot et al.⁸ for details. In Foot et al.⁸ two quantities have been introduced to perform a χ^2 analysis. One is the double ratio^{15,10}

$$R \equiv \frac{(N_\mu/N_e)|_{\text{osc}}}{(N_\mu/N_e)|_{\text{no-osc}}}$$

where the quantities $N_{e,\mu}$ are the numbers of e -like and μ -like events. The numerator denotes numbers with oscillation probability obtained by (1), while the denominator the numbers expected with oscillations switched off. The other one is the quantity on up-down flux asymmetries for α -like ($\alpha=e,\mu$) events and is defined by

$$Y_\alpha \equiv \frac{(N_\alpha^{-0.2}/N_\alpha^{+0.2})|_{\text{osc}}}{(N_\alpha^{-0.2}/N_\alpha^{+0.2})|_{\text{no-osc}}},$$

where $N_\alpha^{-\eta}$ denotes the number of α -like events produced in the detector with zenith angle $\cos \Theta < -\eta$, while $N_\alpha^{+\eta}$ denotes the analogous quantity for $\cos \Theta > \eta$, where η is defined to be positive. Superkamiokande divides the $(-1, +1)$ interval in $\cos \Theta$ into five equal bins, so we choose $\eta = 0.2$ in order to use all the data in the other four bins. Thus χ^2 for atmospheric neutrinos is defined by

$$\chi_{\text{atm}}^2 = \sum_E \left[\left(\frac{R^{SK} - R^{\text{th}}}{\delta R^{SK}} \right)^2 + \left(\frac{Y_\mu^{SK} - Y_\mu^{\text{th}}}{\delta Y_\mu^{SK}} \right)^2 + \left(\frac{Y_e^{SK} - Y_e^{\text{th}}}{\delta Y_e^{SK}} \right)^2 \right],$$

where the sum is over the sub-GeV and multi-GeV cases, the measured Superkamiokande values and errors are denoted by the superscript “SK” and the theoretical predictions for the quantities are labeled by “th”. In Foot et al.⁸ a χ^2 analysis has been performed using the quantities R and Y ’s, or using Y ’s only. Throughout this paper we use the quantities R and Y ’s to get narrower allowed regions for the parameters. We have to incorporate also the results of the reactor experiments. We define the following χ^2 :

$$\chi_{\text{reactor}}^2 = \sum_{j=1,12}^{\text{CHOOZ}} \left(\frac{x_j - y_j}{\delta x_j} \right)^2 + \sum_{j=1,60}^{\text{Bugey}} \left(\frac{x_j - y_j}{\delta x_j} \right)^2 + \sum_{j=1,8}^{\text{Krasnoyarsk}} \left(\frac{x_j - y_j}{\delta x_j} \right)^2,$$

where x_i are experimental values and y_i are the corresponding theoretical predictions, and the sum is over 12, 60, 8 energy bins of data of CHOOZ², Bugey¹ and Krasnoyarsk²⁷, respectively. There are 6 atmospheric and 80 reactor pieces of data in $\chi^2 \equiv \chi_{\text{atm}}^2 + \chi_{\text{reactor}}^2$ and 3 adjustable parameters, m^2 , θ_{13} and θ_{23} , leaving 83 degrees of freedom.

The best fit is obtained for $(m^2, \tan^2 \theta_{13}, \tan^2 \theta_{23}, \chi^2) = (7 \times 10^{-3} \text{ eV}^2, 1.1 \times 10^{-2}, 0.93, 71.8)$ for $m^2 > 0$ and $(-7 \times 10^{-3} \text{ eV}^2, 1.5 \times 10^{-2}, 1.1, 71.4)$

for $m^2 < 0$, respectively. $\chi^2_{\min} = (\chi^2_{\text{atm}})_{\min} + (\chi^2_{\text{reactor}})_{\min} = 4.2 + 67.2 = 71.4$ indicates that a fit to data is good for 83 degrees of freedom at the best fit point. The allowed region for m^2 with θ_{13}, θ_{23} unconstrained is given in Fig. 2, where $\Delta\chi^2 \equiv \chi^2_{\text{atm}} + \chi^2_{\text{reactor}} - (\chi^2_{\text{atm}} + \chi^2_{\text{reactor}})_{\min} < 3.5, 6.3, 11.5$ corresponds to 1σ , 90 % CL and 99 % CL, respectively. The allowed region for $|m^2|$ at 99% CL is $4 \times 10^{-4} \text{ eV}^2 \lesssim |m^2| \lesssim 1.7 \times 10^{-2} \text{ eV}^2$.

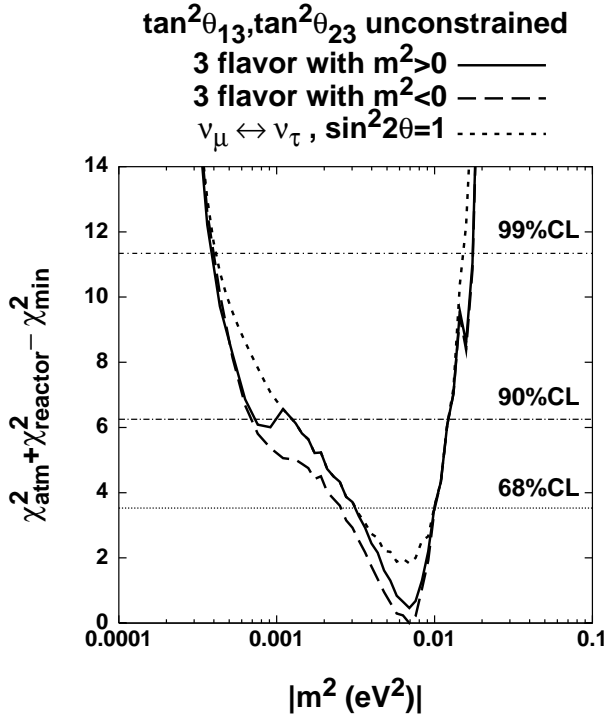


Fig. 2
Value of $\Delta\chi^2 \equiv \chi^2_{\text{atm}} + \chi^2_{\text{reactor}} - (\chi^2_{\text{atm}} + \chi^2_{\text{reactor}})_{\min} = \chi^2_{\text{atm}} + \chi^2_{\text{reactor}} - 71.4$. The solid, dash-dotted, dotted lines represent the scenarios (a), (b) and the two flavor case with maximal $\nu_\mu \leftrightarrow \nu_\tau$ mixing, respectively.

Using the same parametrization as that in Fogli et al.⁵, the results for the allowed region of the mixing angles (θ_{13}, θ_{23}) are given for various values of m^2 in Figs. 3 and 4. The results for $m^2 > 0$ (Fig. 3) and $m^2 < 0$ (Fig. 4) are almost the same. Notice that θ_{13} can be large in the region of m^2 where the CHOOZ data² give no constraint on θ_{13} .

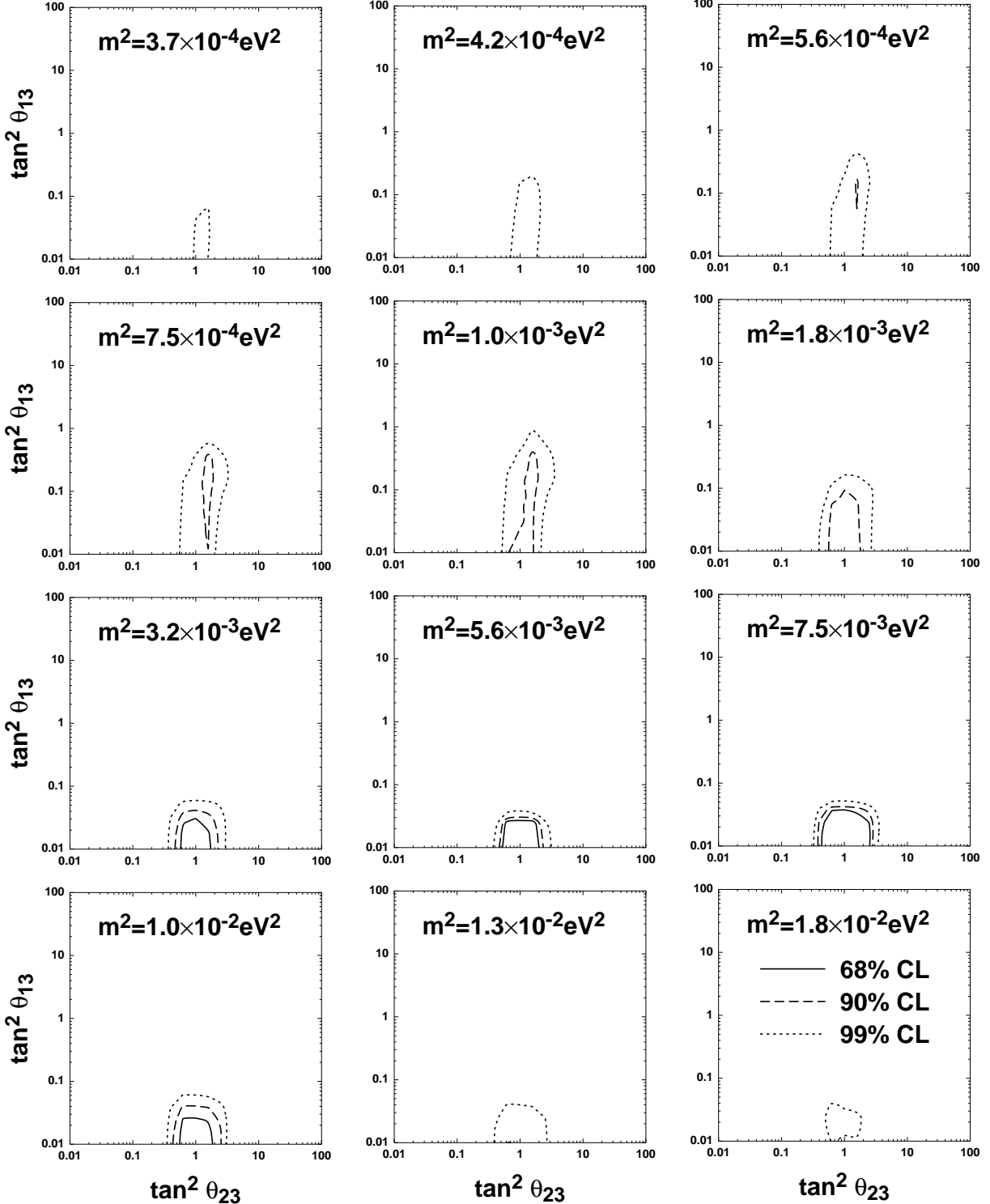


Fig. 3 The solid, dashed, dotted lines represent the allowed region at 68 % CL, 90 % CL, 99 % CL, respectively for scenario (a) in Fig. 1.

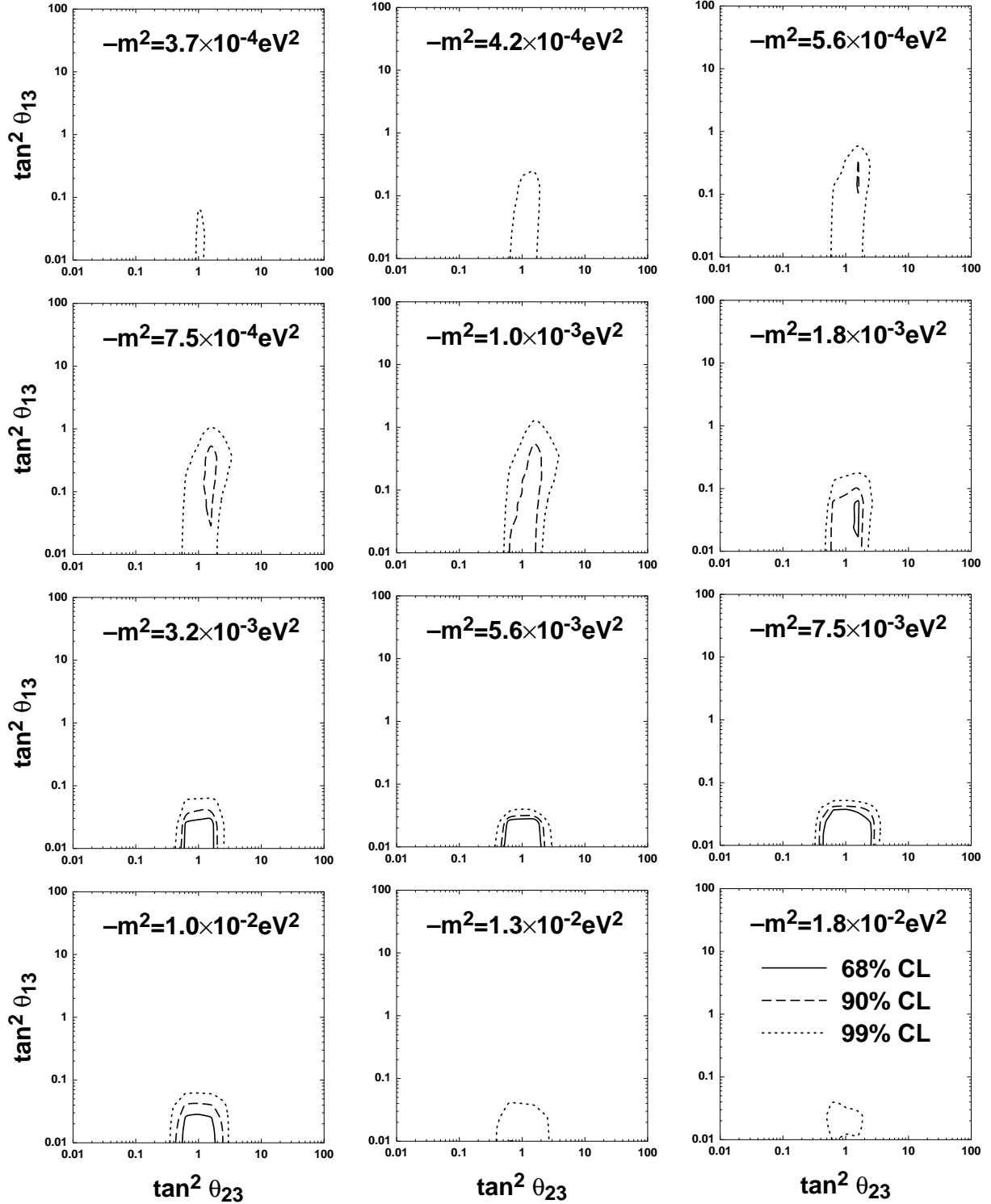


Fig. 4 As in Fig. 3, but the scenario (b) in Fig. 1 is assumed.

3. The implications to the long baseline experiments

In the present case with mass scale hierarchy the oscillation probability $P(\nu_\mu \rightarrow \nu_e)$ in vacuum is given by

$$P(\nu_\mu \rightarrow \nu_e) = 4|U_{e3}|^2|U_{\mu 3}|^2 \sin^2 \left(\frac{\Delta m_{31}^2 L}{4E} \right) = s_{23}^2 \sin^2 2\theta_{13} \sin^2 \left(\frac{m^2 L}{4E} \right),$$

so that we observe that the factor $4|U_{e3}|^2|U_{\mu 3}|^2$ corresponds to $\sin^2 2\theta$ in the two flavor framework. For each m^2 in Figs. 3 and 4 the maximal allowed values of $4|U_{e3}|^2|U_{\mu 3}|^2$ have been evaluated and are shown in Figs. 5(a) and 5(b) in the two flavor plot ($\sin^2 2\theta, \Delta m^2$), respectively, where the regions which can be probed by K2K²³, MINOS²¹ and KamLAND^{26,25} are also given. The only promising channel for the K2K experiment is $\nu_\mu \leftrightarrow \bar{\nu}_\mu$ disappearance, while MINOS might have a chance to see $\nu_\mu \rightarrow \nu_e$ appearance and KamLAND may be also able to observe $\bar{\nu}_e \leftrightarrow \bar{\nu}_e$ disappearance.

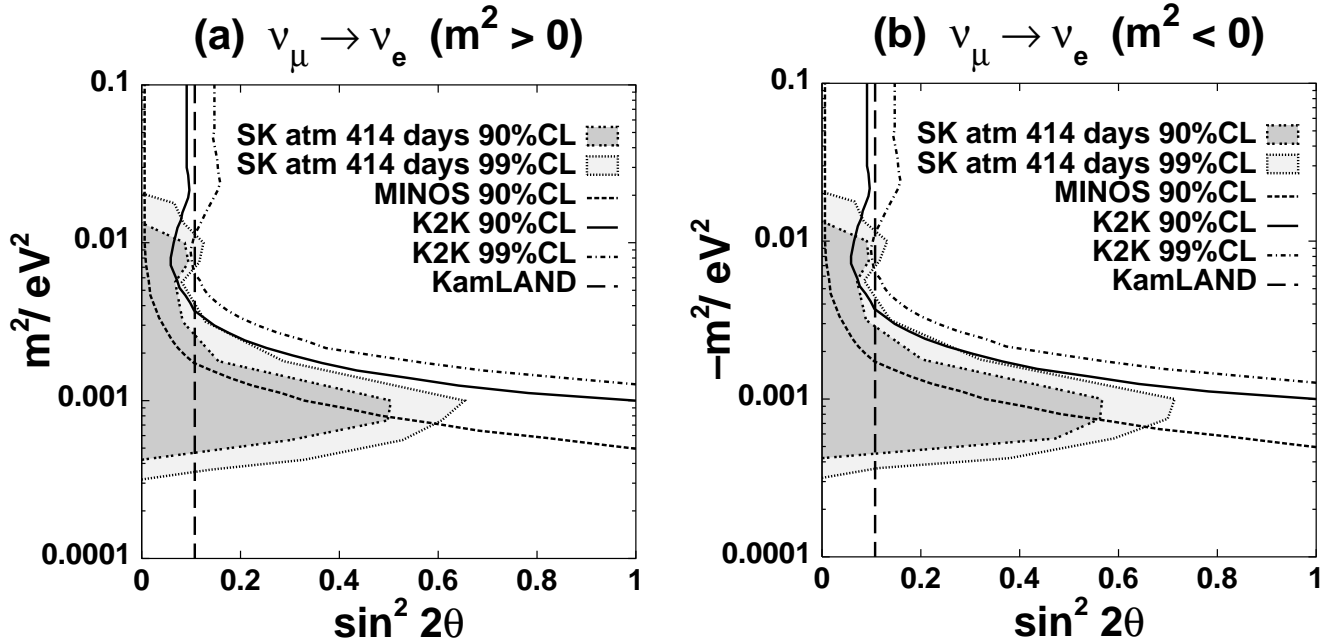


Fig. 5

Shadowed regions are allowed from the Superkamiokande atmospheric neutrino data for the scenario (a) (Fig. 5(a)) or (b) (Fig. 5(b)) in Fig. 1, respectively. The region which can be probed by the long baseline experiments (K2K, MINOS, KamLAND) is the right side of each line.

4. The threefold maximal mixing model^{22,14,13}

Using (1) and (3), and redefining $\nu_e \rightarrow e^{i\delta} \nu_e$ we have

$$\begin{aligned}
& i \frac{d}{dx} \begin{pmatrix} \nu_e(x) \\ \nu_\mu(x) \\ \nu_\tau(x) \end{pmatrix} \\
&= e^{i\theta_{23}\lambda_7} \left[e^{i\theta_{13}\lambda_5} \text{diag}(0, 0, \Delta E_{31}) e^{-i\theta_{13}\lambda_5} + \text{diag}(A, 0, 0) \right] e^{-i\theta_{23}\lambda_7} \begin{pmatrix} \nu_e(x) \\ \nu_\mu(x) \\ \nu_\tau(x) \end{pmatrix} \\
&= e^{i\theta_{23}\lambda_7} e^{i\theta_M\lambda_5} \left[\frac{\Delta E_{31} + A}{2} \text{diag}(1, 0, 1) - \frac{B}{2} \text{diag}(1, 0, -1) \right] e^{-i\theta_M\lambda_5} e^{-i\theta_{23}\lambda_7} \begin{pmatrix} \nu_e(x) \\ \nu_\mu(x) \\ \nu_\tau(x) \end{pmatrix}, \tag{4}
\end{aligned}$$

where θ_M is the mixing angle in matter given by

$$\tan 2\theta_M \equiv \frac{\Delta E_{31} \sin 2\theta_{13}}{\Delta E_{31} \cos 2\theta_{13} - A}$$

as in the two flavor case^{20,28} , and

$$B \equiv \sqrt{(\Delta E_{31} \cos 2\theta_{13} - A)^2 + (\Delta E_{31} \sin 2\theta_{13})^2}.$$

If we assume that the density of the Earth is approximately constant, then (4) can be integrated as

$$\begin{pmatrix} \nu_e(L) \\ \nu_\mu(L) \\ \nu_\tau(L) \end{pmatrix} = e^{i\theta_{23}\lambda_7} e^{i\theta_M\lambda_5} \text{diag} \left(e^{-i\Phi}, 1, e^{-i\Psi} \right) e^{-i\theta_M\lambda_5} e^{-i\theta_{23}\lambda_7} \begin{pmatrix} \nu_e(0) \\ \nu_\mu(0) \\ \nu_\tau(0) \end{pmatrix},$$

where

$$\left\{ \begin{array}{c} \Phi \\ \Psi \end{array} \right\} = \frac{L}{2} (\Delta E_{31} + A \mp B).$$

The oscillation probability is given by

$$\begin{aligned}
P(\nu_e \rightarrow \nu_e) &= 1 - \sin^2 2\theta_M \sin^2 \frac{\Phi - \Psi}{2} \\
P(\nu_e \rightarrow \nu_\mu) &= s_{23}^2 \sin^2 2\theta_M \sin^2 \frac{\Phi - \Psi}{2} \\
P(\nu_\mu \rightarrow \nu_\mu) &= 1 - s_{23}^4 \sin^2 2\theta_M \sin^2 \frac{\Phi - \Psi}{2} - \sin^2 2\theta_{23} \left(s_M^2 \sin^2 \frac{\Phi}{2} + c_M^2 \sin^2 \frac{\Psi}{2} \right) \tag{5}
\end{aligned}$$

One of the interesting applications is the behaviors of the oscillation probability (5) in the three flavor maximal mixing model^{22,14,13}, which is obtained by putting $\theta_{12} = \theta_{23} = \pi/4$, $\theta_{13} = \sin^{-1}(1/\sqrt{3})$, $\delta = \pi/2$ in the present parametrization. If $|\Delta E_{31}| \ll A$ then we see from (5) that the mixing angle θ_M becomes $\pi/2$, so we get from (5)

$$\begin{aligned} P(\nu_e \rightarrow \nu_e) &\simeq 1 \\ P(\nu_\mu \rightarrow \nu_\mu) &\simeq 1 - \sin^2 2\theta_{23} \sin^2 \frac{\Phi}{2} = 1 - \sin^2 \frac{\Phi}{2}, \end{aligned} \quad (6)$$

where we have used the fact

$$\Phi \simeq \frac{\Delta E_{31} L}{2} (1 + \cos 2\theta_{13}) = c_{13}^2 \Delta E_{31} L = \frac{2}{3} \Delta E_{31} L.$$

(6) indicates that the mixing becomes pure $\nu_\mu \leftrightarrow \nu_\tau$ with maximal mixing and this is why a fit of this model to the data becomes reasonably good for lower Δm_{31}^2 ⁹. On the other hand, if $|\Delta E_{31}| \gg A$, then θ_M becomes θ_{13} and we find again from (5)

$$\begin{aligned} P(\nu_e \rightarrow \nu_e) &\simeq 1 - \frac{1}{2} \sin^2 2\theta_{13} = \frac{5}{9} \\ P(\nu_\mu \rightarrow \nu_\mu) &\simeq 1 - \frac{1}{2} s_{23}^4 \sin^2 2\theta_{13} - \sin^2 2\theta_{23} \left(s_{13}^2 \sin^2 \frac{AL}{3} + \frac{1}{2} c_{13}^2 \right) \\ &= \frac{5}{9} - \frac{1}{3} \sin^2 \frac{AL}{3}, \end{aligned}$$

where we have used

$$\Phi \simeq \frac{\Delta AL}{2} (1 + \cos 2\theta_{13}) = c_{13}^2 AL = \frac{2}{3} AL.$$

Possibility with larger Δm_{31}^2 is excluded by the CHOOZ result², but a fit of this model to the atmospheric neutrino data themselves is reasonably good because of the factor $\sin^2(AL/3)$ accounts for the zenith angle dependence to some extent^{6,9}. These two behaviors can be confirmed numerically as is shown in Fig. 6 where the value of χ^2_{CHOOZ} is also plotted. Thus we see the analytic formulae for constant density explain the qualitative behaviors of the oscillation probability well. The threefold maximal mixing model fits to the data of atmospheric neutrinos and the CHOOZ experiment for $m^2 \simeq 8 \times 10^{-4} \text{ eV}^2$ ⁹.

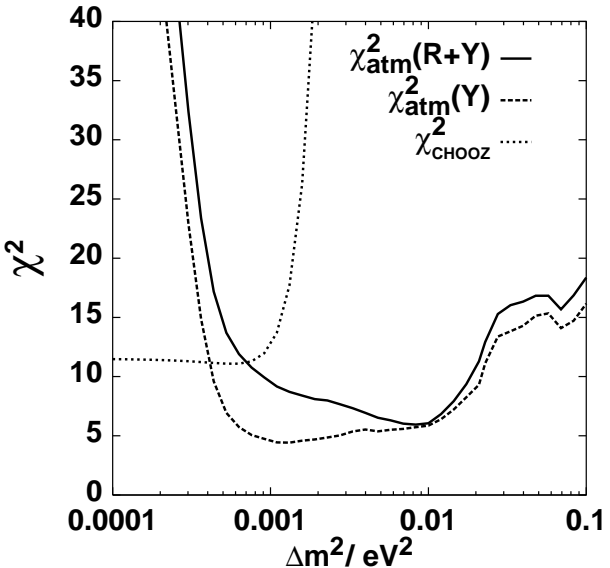


Fig. 6
 χ^2 fit as a function of Δm^2 to the Superkamiokande atmospheric data for the threefold maximal mixing model. The solid line includes both R and up-down asymmetries whereas the dashed line includes only the up-down asymmetries (# of degrees of freedom = 6–1=5 for $R+Y$ and =4–1=3 for Y only). The χ^2 for the CHOOZ reactor data (dotted line; # of degrees of freedom = 12–1=11) is also shown.

5. Conclusions

I have presented a result on the three flavor analysis of the Superkamiokande atmospheric neutrino data for 414 days. If the mass squared difference is smaller than $1 \times 10^{-3} \text{ eV}^2$ then there can be large mixing between ν_μ and ν_e . It was shown that K2K will be able to see only $\nu_\mu \leftrightarrow \bar{\nu}_\mu$ disappearance, while there may be a chance for MINOS (KamLAND) to see $\nu_\mu \rightarrow \nu_e$ appearance ($\bar{\nu}_e \leftrightarrow \bar{\nu}_e$ disappearance), respectively. The threefold maximal mixing model gives a reasonable fit to the atmospheric neutrino and CHOOZ data for $\Delta m^2 \sim 1 \times 10^{-3} \text{ eV}^2$. It should be emphasized that the matter effects are important in the analysis of atmospheric neutrinos.

Acknowledgement

The author would like to thank H. Minakata and E. Lisi for discussions, R. Foot and R.R. Volkas for collaboration and discussions. This research was supported in part by a Grant-in-Aid for Scientific Research of the Ministry of Education, Science and Culture, #09045036, #10140221, #10640280.

6. References

1. B. Ackar et al., 1995, Nucl. Phys. **B434**, 503.
2. M. Apollonio et al., 1998, Phys. Lett. **B420**, 397.
3. See, e.g., J.N. Bahcall, R. Davis, Jr., P. Parker, A. Smirnov, R. Ulrich eds., 1994, *SOLAR NEUTRINOS: the first thirty years* Reading, Mass., Addison-Wesley and references therein.
4. V. Barger, K. Whisnant, S. Pakvasa and R.J.N. Phillips, 1980, Phys. Rev. **D22**, 2718.
5. G.L. Fogli, E. Lisi, D. Montanino and G. Scioscia, 1997, Phys. Rev. **D55**, 4385.
6. G. L. Fogli, E. Lisi, A. Marrone, and D. Montanino, 1998, Phys. Lett. **B425**, 341.
7. G. L. Fogli, E. Lisi, A. Marrone, and G. Scioscia, 1998, hep-ph/9808205.
8. R. Foot, R. R. Volkas and O. Yasuda, 1998, Phys. Rev. **D58**, 13006.
9. R. Foot, R. R. Volkas and O. Yasuda, 1998, Phys. Lett. **B433**, 82.
10. Y. Fukuda et al., 1994, Phys. Lett. **B335**, 237.
11. Y. Fukuda et al., 1998, Phys. Lett. **B433**, 9; 1998, hep-ex/9805006.
12. Y. Fukuda et al., 1998, hep-ex/9807003.
13. C. Giunti, C. W. Kim and J. D. Kim, 1995, Phys. Lett. **B352**, 357.
14. P. F. Harrison, D. H. Perkins and W. G. Scott, 1995, Phys. Lett. **B349**, 137; 1997, Phys. Lett. **B396**, 186.
15. K. S. Hirata et al., 1992, Phys. Lett. **B280**, 146.
16. ICARUS experiment, <http://www.aquila.infn.it/icarus/>.
17. T. Kajita, Talk at *XVIII International Conference on Neutrino Physics and Astrophysics*, June, 1998, Takayama, Japan
(<http://www-sk.icrr.u-tokyo.ac.jp/nu98/scan/063/>).
18. E. Lisi, Talk at *New Era in Neutrino Physics*, June, 1998, Tokyo Metropolitan University, Japan
(<http://musashi.phys.metro-u.ac.jp/neutrino/june12/e-lisi/>).
19. Z. Maki, M. Nakagawa and S. Sakata, 1962, Prog. Theor. Phys. **28**, 870.
20. S. P. Mikheyev and A. Smirnov, 1986, Nuovo Cim. **9C**, 17.
21. MINOS experiment, <http://www.hep.anl.gov/NDK/HyperText/numi.html>.
22. R. N. Mohapatra and S. Nussinov, 1995, Phys. Lett. **B346**, 75.
23. K. Nishikawa, preprint INS-Rep.924 (1992); Talk at *XVIII International Conference on Neutrino Physics and Astrophysics*, June, 1998, Takayama, Japan
(<http://www-sk.icrr.u-tokyo.ac.jp/nu98/scan/093/>).
24. Particle Data Group, 1998, Eur. Phys. J. **C3**, 1.

25. F. Suekane, Talk at *New Era in Neutrino Physics*, June, 1998, Tokyo Metropolitan University, Japan
(<http://musashi.phys.metro-u.ac.jp/neutrino/june12/f-suekane/>).
26. A. Suzuki, Talk at *XVIII International Conference on Neutrino Physics and Astrophysics*, June, 1998, Takayama, Japan
(<http://www-sk.icrr.u-tokyo.ac.jp/nu98/scan/083/>).
27. G. S. Vidyakin et al., 1994, JETP Lett. **59**, 390.
28. L. Wolfenstein, 1978, Phys. Rev. **D17**, 2369.